

Two-dimensional electron gases in strained quantum wells for AlN/GaN/AlN double heterostructure field-effect transistors on AlN

Guowang Li, Bo Song, Satyaki Ganguly, Mingda Zhu, Ronghua Wang, Xiaodong Yan, Jai Verma, Vladimir Protasenko, Huili Grace Xing, and Debdeep Jena^{a)}

Department of Electrical Engineering, University of Notre Dame, Indiana 46556, USA

(Received 24 March 2014; accepted 27 April 2014; published online 14 May 2014)

Double heterostructures of strained GaN quantum wells (QWs) sandwiched between relaxed AlN layers provide a platform to investigate the quantum-confined electronic and optical properties of the wells. The growth of AlN/GaN/AlN heterostructures with varying GaN quantum well thicknesses on AlN by plasma molecular beam epitaxy (MBE) is reported. Photoluminescence spectra provide the optical signature of the thin GaN QWs. Reciprocal space mapping in X-ray diffraction shows that a GaN layer as thick as ~ 28 nm is compressively strained to the AlN layer underneath. The density of the polarization-induced two-dimensional electron gas (2DEG) in the undoped heterostructures increases with the GaN QW thickness, reaching $\sim 2.5 \times 10^{13}/\text{cm}^2$. This provides a way to tune the 2DEG channel density without changing the thickness of the top barrier layer. Electron mobilities less than ~ 400 cm^2/Vs are observed, leaving ample room for improvement. Nevertheless, owing to the high 2DEG density, strained GaN QW field-effect transistors with MBE regrown ohmic contacts exhibit an on-current density ~ 1.4 A/mm, a transconductance ~ 280 mS/mm, and a cut off frequency $f_T \sim 104$ GHz for a 100-nm-gate-length device. These observations indicate high potential for high-speed radio frequency and high voltage applications that stand to benefit from the extreme-bandgap and high thermal conductivity of AlN. © 2014 AIP Publishing LLC.

[<http://dx.doi.org/10.1063/1.4875916>]

Wide bandgap III-Nitride semiconductor heterostructures for electronic device applications have been mostly limited to GaN substrates. For high-speed microwave and high-voltage power electronics applications, various heterostructures such as AlGaN/GaN or InAlN/GaN sit on a thick GaN (or low Al composition AlGaN) buffer layer.^{1–5} These thick GaN buffer layers are either in the bulk GaN form or grown epitaxially on sapphire, SiC, or Silicon with defects. The conductive channels are two-dimensional electron gases (2DEGs) at the heterojunctions. Various design constraints exist—for example, to change the 2DEG density, one must change the barrier thickness. For high electron mobility transistors (HEMTs) on Silicon, the GaN buffer layers have to be very thick to prevent high electric fields from reaching the Silicon causing premature breakdown.⁶

In this work, we show that moving to *thin* and *strained* GaN quantum wells (QWs) surrounded by AlN buffer and barrier layers are a feasible and attractive approach for electronic applications. The extreme-bandgap ($E_g \sim 6.2$ eV), electrical insulating characteristics, and high thermal conductivity ($\kappa \sim 300$ W/mK (Ref. 7)) of AlN brings about a number of opportunities and removes some of the constraints of being on a GaN platform. The device structures demonstrated in this work have very little GaN in them.

AlN has a large conduction band offset with GaN, and a large difference in polarization. The combination of the two induces high density 2DEG channels in AlN/GaN heterostructures on GaN substrates where the AlN is strained.⁸ The large band offset provides tight electrostatic and quantum confinement, making AlN very attractive *also as a back-barrier*. The

resulting metal-face AlN/GaN/AlN double heterostructure on *AlN substrates* is of great interest as a material platform to investigate electronic and optical properties of the isolated and confined GaN QW. In these heterostructures, the GaN QW is strained, and the AlN buffer and top heterostructure barrier are relaxed. An earlier report showed AlGaN/GaN/AlN double heterostructures with thick *relaxed* GaN channels.¹⁰ In this report, we focus on the material characteristics of the heterostructures and the transport properties of the 2DEG in such double heterostructure strained GaN QWs. The direct current (DC) characteristics of ultrathin body GaN quantum well field-effect transistors (FETs) on AlN were recently demonstrated.¹¹ In this work, we also demonstrate vastly improved DC characteristics and radio frequency (RF) performance with cutoff frequencies exceeding 100 GHz using strained GaN QW FETs on AlN.

The AlN/GaN/AlN double heterostructures were grown on Al-polar semi-insulating AlN templates on sapphire by plasma-assisted molecular beam epitaxy (MBE) in a Veeco Gen 930 system. A ~ 200 -nm-thick unintentionally doped (UID) AlN buffer was epitaxially grown, followed by a thin strained GaN QW to host the 2DEG channel. The GaN QW thickness was varied systematically to investigate the 2DEG transport properties. An AlN layer was grown on the GaN QW as the top barrier and capped with a thin GaN layer to prevent oxidation of the AlN surface. The AlN and GaN layers were grown under metal rich conditions with a Ga flux of $\sim 2.6 \times 10^{-7}$ Torr, an Al flux of $\sim 9 \times 10^{-8}$ Torr, and a RF power of 275 W. The resulting growth rate was ~ 140 nm/h, as inferred from various post-growth characterization techniques. The substrate temperature used was ~ 720 °C for the AlN buffer and ~ 660 °C for the GaN QW

^{a)}Electronic mail: djena@nd.edu

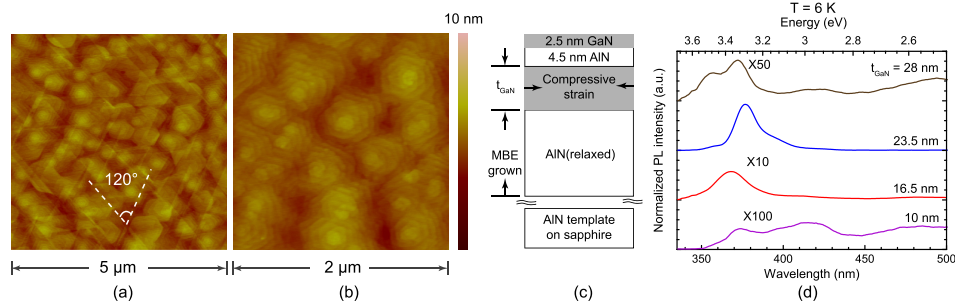


FIG. 1. AFM images showing surfaces of (a) 2.5 nm GaN/10 nm AIN/1.5 μm GaN/SiC substrate and (b) 2.5 nm GaN/10 nm AIN/20 nm GaN/1 μm AIN/sapphire substrate. Cracks were observed on sample (a) but not (b). (c) Schematic of the AIN/GaN/AIN double heterostructures. (d) Photoluminescence spectra of AIN/GaN/AIN double heterostructures with varied GaN QW thicknesses at $T = 6$ K, showing photon emissions from GaN QWs. The PL intensity of the 10, 16.5, and 28 nm GaN QW samples was multiplied by a factor of 100, 10, and 50, respectively.

and the top barriers. An AIN/GaN heterostructure was grown on a SiC substrate as a control sample to illustrate the advantages of the AIN substrate.

A thick AIN top barrier is expected to improve breakdown characteristics of nitride electronic devices.¹⁴ In conventional AIN/GaN heterostructures on GaN template, it is impractical to have AIN top barrier exceeding critical thickness (~ 7 nm)⁸ due to strain-induced relaxation of AIN and the resulting cracks. However, a thick AIN top barrier is enabled by the AIN template and strained GaN QW. To illustrate the benefit of the AIN template for allowing thick AIN top barriers, two heterostructures were grown with the same AIN top barrier thickness of 10 nm but on different templates: (a) a control sample of 2.5 nm GaN/10 nm AIN/1.5 m GaN/SiC substrate and (b) a QW sample of 2.5 nm GaN/10 nm AIN/20 nm GaN/1 m AIN/sapphire substrate. The atomic force microscope (AFM) scans of the surface morphology of (a) the control sample and (b) the AIN/GaN/AIN QW sample are shown in Fig. 1(a) and Fig. 1(b), respectively. Fig. 1(a) shows the expected cracks on the control sample. For the sample (b) grown on the AIN template, no cracks were observed, indicating that the GaN QW is strained to the AIN buffer. Furthermore, the surface is very smooth, characterized by an rms roughness of ~ 0.3 nm for the 2×2 μm scan. The smooth surface is attractive for device processing and uniformity.

Fig. 1(c) shows the schematic layer structures of the AIN/GaN/AIN double heterostructures used for the rest of the report. The thickness t_{GaN} of the GaN QW, which is under

compressive strain, is varied from 5 to 33 nm. Fig. 1(d) shows the 6 K photoluminescence (PL) spectra of AIN/GaN/AIN double heterostructures with varying GaN QW thicknesses, excited by a 325 nm He-Cd laser. Photon emission from the GaN QW is observed for all four samples. The GaN QW PL emission peaks at 374, 368, 377, and 372 nm for the 10, 16.5, 23, and 28 nm samples, respectively. The peak wavelengths and intensities are determined by quantized states in the well, the interplay of red or blue shifts determined by the polarization-induced quantum-confined Stark effect (QCSE), varying oscillator strengths, and the net optically active GaN material. A detailed analysis of the PL spectra is not attempted here, and is proposed for future work. For the rest of this report, we focus on the structural and transport properties of the heterostructures.

High-resolution X-ray diffraction (XRD) measurements were performed on the samples with varying GaN QW thicknesses. The top barriers for all samples were 2.5/4.5 nm GaN/AIN except for the AIN buffer control sample. Symmetric (002) reflection spectra in Fig. 2(a) shows the evolution of the GaN QW peak: the intensity of the GaN QW increases and the full width at half maximum (FWHM) decreases with the QW thickness. To investigate the strain state in the GaN QW, a 28-nm-thick GaN QW sample was examined by reciprocal space mapping (RSM) around the asymmetric (105) reflection, as shown in Fig. 2(b). Two dashed lines for coherently strained ($R = 0$) and fully relaxed ($R = 1$) layers on AIN are included.¹² This RSM image shows that the GaN layer is strained to the AIN lattice

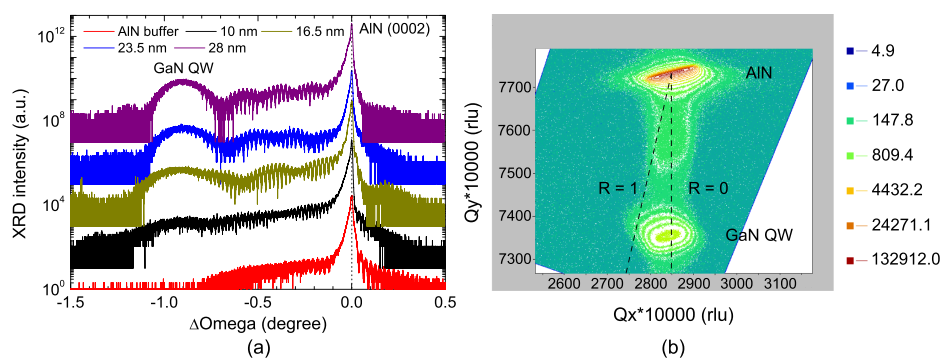


FIG. 2. Symmetric (002) reflection spectra of AIN buffer (without GaN QW and top barriers) and AIN/GaN/AIN double heterostructures with varied GaN QW thicknesses, measured by high-resolution X-ray diffraction. (b) Reciprocal space mapping for the asymmetric (105) reflections of a 28-nm-thick GaN QW sample, showing the GaN QW is strained to AIN buffer. Two lines representing coherently strained ($R = 0$) and fully relaxed ($R = 1$) layers on AIN are also included.

constant. The extracted lattice constants (a , c) are ($a_{\text{AlN}} = 3.122 \text{ \AA}$, $c_{\text{AlN}} = 4.981 \text{ \AA}$) and ($a_{\text{GaN}} = 3.132 \text{ \AA}$, $c_{\text{GaN}} = 5.237 \text{ \AA}$), respectively. Compared to bulk (unstrained) lattice constants ($a_{0(\text{AlN})} = 3.112 \text{ \AA}$, $c_{0(\text{AlN})} = 4.982 \text{ \AA}$) and ($a_{0(\text{GaN})} = 3.189 \text{ \AA}$, $c_{0(\text{GaN})} = 5.186 \text{ \AA}$),¹³ the GaN QW is in $\sim 1.78\%$ compressive strain, and the AlN buffer is in $\sim 0.33\%$ tensile strain. The relaxation of the GaN QW with respect to the AlN buffer is of $(a_{\text{GaN}} - a_{0(\text{AlN})})/a_{0(\text{GaN})} - a_{0(\text{AlN})} \sim 26\%$. In contrast to the small critical thickness ($\sim 7 \text{ nm}$) of AlN on GaN substrate, ~ 4 times thicker GaN layer could be grown on AlN and remains strained. This enables tuning the GaN QW thickness without losing the benefits of strained heterostructures (e.g., thick top AlN barrier for higher 2DEG density).

The electronic properties of the AlN/GaN/AlN double heterostructures were modeled using a self-consistent Poisson-Schrödinger solver.¹⁵ Fig. 3(a) shows the simulated energy band diagrams and the electron distributions for the 15/30 nm GaN QW samples, with a surface barrier height of 1 eV. The two heterojunctions at the top and bottom hetero-interfaces of the GaN QW with AlN consists a fixed sheet charge dipole due to the polarization charge discontinuity between AlN and GaN. As the distance between the sheet charges of the dipole decreases with the QW thickness, the electric field in the well increases to confine electrons more tightly near the top heterojunction, and the 2DEG density decreases. Hall-effect measurements were performed at room temperature (RT) and 77 K with In dot Ohmic contacts to the QW 2DEGs. The dependence of measured 2DEG density and mobility on the GaN QW thickness is shown in Fig. 3(b). The simulated trend of 2DEG density is also included, in agreement with the measured data. The discrepancy between the data of the 33-nm-thick sample and simulation may be due to the relaxation of the GaN QW. The piezoelectric polarization charge induced by the compressive strain in GaN layer is opposite to the spontaneous polarization charge. If the GaN QW is relaxed, the 2DEG density is expected to be higher than that in the strained case.

Unlike AlN/GaN heterostructures on GaN substrates, the 2DEG in the AlN/GaN/AlN double heterostructure is influenced by the bound negative polarization sheet charge at the bottom GaN/AlN heterojunction. This results in the dependence of transport properties on the quantum well thickness, which has been reported for AlGaIn/GaN/AlGaIn double heterostructures.⁹ As shown in Fig. 3(b), with the same top barrier thicknesses in all heterostructures, the

2DEG density can be changed by varying the QW thickness from $\sim 1.2 \times 10^{13}/\text{cm}^2$ to $\sim 2.5 \times 10^{13}/\text{cm}^2$. This is in stark contrast to AlGaIn/GaN 2DEGs, where the 2DEG density depends on the barrier thickness. This heterostructure enables other capabilities. For example, normally off operation could be enabled in 5-nm-thick GaN QW samples (not shown), which were highly resistive in the Hall-effect measurement. This is without compromising the thickness or the bandgap of the top barrier, but requires one to form self-aligned contacts. The 2DEG mobility remained below $\sim 400 \text{ cm}^2/\text{Vs}$ at RT, which is lower than that of conventional GaN HEMTs. The mobility is expected to improve with better control of the growth conditions and by the reduction of dislocations and defects from the substrate, which can be achieved by moving to bulk single-crystal AlN substrates. Another possibility for the observation of the low effective Hall-effect mobilities is the possible presence of a 2D hole gas in the quantum well.

The energy band-diagram simulation in Fig. 3(a) also shows that a two-dimensional hole gas (2DHG) must form at the bottom heterojunction in the ideal case. We recently reported the observation of a very high density 2DHG due to the negative polarization charge in similar GaN/AlN heterostructures, but *without* the AlN top barrier layers.¹⁶ No direct evidence of the 2DHG was observed in the Hall-effect measurements in the AlN/GaN/AlN double heterostructure samples reported here. It is possible that the Hall-effect measurement is sampling parallel electron-hole bilayer transport, but more careful transport analysis—for example, using quantitative mobility spectrum analysis (QMSA) can help uncover such ambipolar transport behavior. Such a measurement has not been performed on these heterostructures yet. A possible way to intentionally induce a 2DHG at the bottom heterojunction while keeping the 2DEG at the top heterojunction is by incorporating Mg modulation dopants. Such heterostructures with electron-hole bilayers in close proximity can potentially exhibit phenomena—such as Coulomb drag and correlated transport—and will be explored in the future.

The AlN template used here is on sapphire. The high thermal conductivity of bulk AlN substrates will enable efficient heat dissipation of RF and high-voltage transistors. The high breakdown field of AlN makes it an attractive substrate platform in nitride power electronics. To illustrate the capability of the AlN/GaN/AlN strained QWs, FETs were fabricated and studied. For the device fabrication, a 30 nm GaN

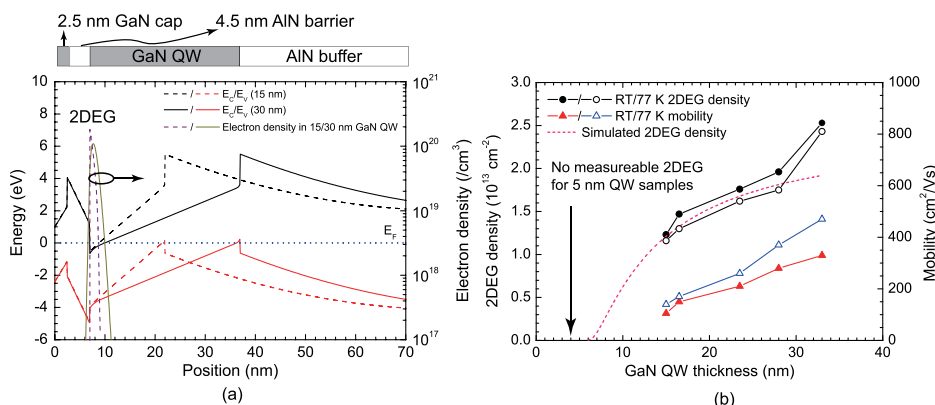


FIG. 3. (a) Energy band diagrams and electron distributions of 15/30 nm GaN QW heterostructures by self-consistent Poisson-Schrödinger simulations. (b) The 2DEG density and mobility measured at RT and 77 K as a function of the GaN QW thickness; the top barriers were fixed as 2.5/4.5 nm GaN/AlN. The simulated trend of 2DEG density is also included.

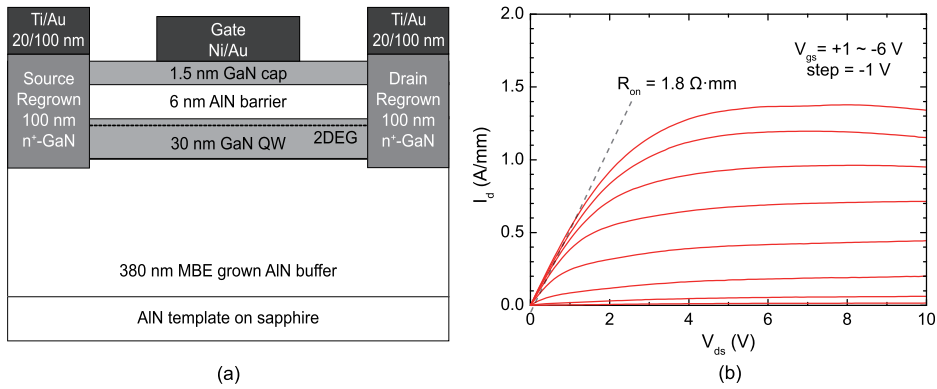


FIG. 4. (a) Schematic cross-sectional view of the GaN QW devices with regrown Ohmic contacts. (b) DC output characteristics of a 30-nm-thick GaN QW device with 1.5/6 nm GaN/AlN top barriers.

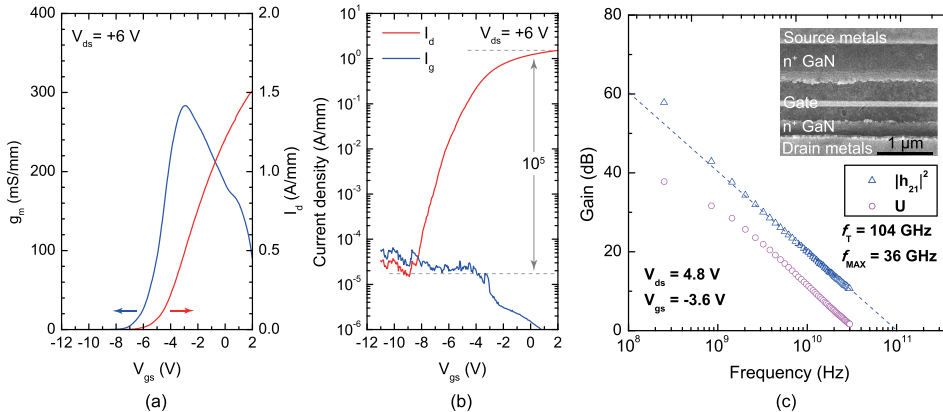


FIG. 5. (a) Linear scale and (b) semilog scale transfer characteristics of the 30-nm-thick GaN QW device at $V_{ds} = 6$ V. (c) RF performance of the 100-nm-gate-length device. Inset shows an SEM image of the device with dimensions of $L_{sd} \sim 650$ nm and $L_{gs} \sim 300$ nm.

QW and 1.5/6 nm GaN/AlN top barrier heterostructure was chosen. The RT 2DEG density of this structure was $\sim 2.2 \times 10^{13}/\text{cm}^2$, and the mobility ~ 310 cm²/Vs with a sheet resistance of ~ 920 Ω/\square measured by Hall-effect. MBE regrowth process was employed for forming low-resistance Ohmic contacts (~ 0.1 $\Omega \cdot \text{mm}$) to the QW 2DEG channel.¹¹ The schematic cross-sectional view of the devices with regrown Ohmic contacts is shown in Fig. 4(a). 100-nm-long gates were defined by electron beam lithography. The family of $I_d - V_{ds}$ curves of the QW FET is shown in Fig. 4(b). A saturation drain current of ~ 1.4 A/mm is observed, even on the AlN-on-sapphire substrate. The on-resistance is $R_{on} \sim 1.8$ $\Omega \cdot \text{mm}$ in the linear region, dominated by the access resistances between the gate-source and gate-drain regions. Self-heating¹⁷ was observed due to the poor thermal conductivity of the sapphire substrates. Bulk AlN substrates with better heat dissipation will significantly boost the device performance. The linear and semilog scale transfer characteristics of the 30-nm-thick GaN QW device at $V_{ds} = 6$ V are shown in Figs. 5(a) and 5(b), respectively. The peak extrinsic transconductance reaches ~ 280 mS/mm, with the current on/off ratio exceeding five orders of magnitude. From the scanning electron microscope (SEM) image in Fig. 5(c), device dimensions of $L_g \sim 100$ nm, $L_{sd} \sim 650$ nm and $L_{gs} \sim 300$ nm were measured. The cut off and maximum oscillation frequencies (f_T , f_{MAX}) were measured to be 104 GHz and 36 GHz. The short-circuit current gain ($|h_{21}|^2$) and unilateral gain (U) are plotted in Fig. 5(c). It is surprising that despite the low ($\sim 4 \times$ lower) mobility, the device performance matches that of the conventional 80-nm T-gate AlN/GaN HEMTs on sapphire with similar dimensions.¹⁸ This shows a high potential for RF and high-voltage applications.

In conclusion, we have realized MBE-grown AlN/GaN/AlN double heterostructures with thin and strained GaN quantum wells surrounded by AlN. Thick AlN top barrier was enabled by the AlN template and strained GaN quantum wells with smooth surface. Photon emission from the GaN QW was observed in photoluminescence spectra, and investigation of other optical applications is proposed for future work. The density of the 2DEG could be varied by changing the QW thickness while keeping the top barrier in the heterostructure fixed, which is in contrast to conventional AlGaIn/GaN heterostructures. The transport properties of the 2DEG channel was studied, and the device performance of 100-nm gate length FETs was found to exhibit cutoff frequencies higher than 100 GHz, in spite of low Hall-effect mobilities. The AlN/GaN/AlN heterostructures reported here, thus, form a material system for electronic applications, and at the same time provide a playground for interesting transport physics that has not been seen yet in the III-Nitride material system.

The authors are grateful for partial support of this work from Dr. P. Maki under the ONR THz MURI program, an NSF ECCS grant, and the DARPA Microscale Power Conversion program. This work was also supported in part by the Center for Low Energy Systems Technology (LEAST), one of the six SRC STARnet Centers, sponsored by MARCO and DARPA.

¹U. K. Mishra, P. Parikh, and Y. F. Wu, *Proc. IEEE* **90**, 1022 (2002).

²J. Kuzmik, *IEEE Electron Device Lett.* **22**, 510 (2001).

³D. S. Lee, X. Gao, S. Guo, D. Kopp, P. Fay, and T. Palacios, *IEEE Electron Device Lett.* **32**, 1525 (2011).

- ⁴K. Shinohara, D. Regan, A. Corrión, D. Brown, Y. Tang, J. Wong, G. Candia, A. Schmitz, H. Fung, S. Kim, and M. Micovic, *IEEE Int. Electron Devices Meet.* **2012**, 27.2.1–27.2.4.
- ⁵Y. Yue, Z. Hu, J. Guo, B. Sensale-Rodriguez, G. Li, R. Wang, F. Faria, T. Fang, B. Song, X. Gao, S. Guo, T. Kosel, G. Snider, P. Fay, D. Jena, and H. Xing, *IEEE Electron Device Lett.* **33**, 988 (2012).
- ⁶S. L. Selvaraj, T. Suzue, and T. Egawa, *IEEE Electron Device Lett.* **30**, 587 (2009).
- ⁷G. A. Slack, R. A. Tanzilli, R. O. Pohl, and J. W. Vandersande, *J. Phys. Chem. Solids* **48**, 641 (1987).
- ⁸Y. Cao and D. Jena, *Appl. Phys. Lett.* **90**, 182112 (2007).
- ⁹C. Q. Chen, J. P. Zhang, V. Adivarahan, A. Koudymov, H. Fatima, G. Simin, J. Yang, and M. Asif Khan, *Appl. Phys. Lett.* **82**, 4593 (2003).
- ¹⁰Z. Y. Fan, J. Li, M. L. Nakarmi, J. Y. Lin, and H. X. Jiang, *Appl. Phys. Lett.* **88**, 073513 (2006).
- ¹¹G. Li, R. Wang, J. Guo, J. Verma, Z. Hu, Y. Yue, F. Faria, Y. Cao, M. Kelly, T. Kosel, H. Xing, and D. Jena, *IEEE Electron Device Lett.* **33**, 661 (2012).
- ¹²S. Pereira, M. R. Correia, E. Pereira, K. P. O'Donnell, E. Alves, A. D. Sequeira, N. Franco, I. M. Watson, and C. Deatcher, *Appl. Phys. Lett.* **80**, 3913 (2002).
- ¹³M. Levinshtein, S. Rumyantsev, and M. Shur, *Properties of Advanced Semiconductor Materials: GaN, AlN, InN, BN, SiC, SiGe* (Wiley, New York, 2000).
- ¹⁴J. Joh and J. A. del Alamo, *IEEE Int. Electron Devices Meet.* **2006**, 415–418.
- ¹⁵I. H. Tan, G. L. Snider, L. D. Chang, and E. L. Hu, *J. Appl. Phys.* **68**, 4071 (1990).
- ¹⁶G. Li, R. Wang, B. Song, J. Verma, Y. Cao, S. Ganguly, A. Verma, J. Guo, H. G. Xing, and D. Jena, *IEEE Electron Device Lett.* **34**, 852 (2013).
- ¹⁷R. Gaska, A. Osinsky, J. W. Yang, and M. S. Shur, *IEEE Electron Device Lett.* **19**, 89 (1998).
- ¹⁸K. D. Chabak, D. E. Walker, Jr., M. R. Johnson, A. Crespo, A. M. Dabiran, D. J. Smith, A. M. Wowchak, S. K. Tetlak, M. Kossler, J. K. Gillespie, R. C. Fitch, and M. Trejo, *IEEE Electron Device Lett.* **32**, 1677 (2011).